Table IV. Extended Hückel Parameters Used for the Calculations

atom	orbital	H_{ii}, eV	$\xi_1{}^a$	$\xi_2{}^a$
Co	4s	−9.21	2.0	
	4p	−5.29	2.0	
	3d	−13.18	5.55 (0.5680)	2.10 (0.6060)
P	3s	−18.6	1.6	
	3p	−14.0	1.6	
F	2s	−40.0	2.425	
	2p	−18.1	2.425	
O	2s	−32.3	2.275	
	2p	−14.8	2.275	
N	2s	−26.0	1.95	
	2p	−13.4	1.95	
C	2s	−21.4	1.625	
	2p	−11.4	1.625	
H	1s	−13.6	1.3	

^{a} Two Slater exponents are listed for the 3d functions. Each is followed in parentheses by the coefficient in the double-ζ expansion.

results are quite consistent with theirs (Table III).

We must notice however that Kawamura's radical was very unstable so that it was not possible to obtain a liquid-solution spectrum at room temperature. The isotropic hyperfine tensor value was unknown, leading to an ambiguity concerning the sign

of $A_{\parallel}$ and $A_{\perp}$. Assuming a d_{z^2} ground state, they considered $A_{\parallel}$ as positive and $A_{\perp}$ as negative. Our results provide support to such an interpretation.

The main difference is that they observed a significant anisotropy of the phosphorus coupling constant whereas, in our work, the phosphorus coupling is isotropic within the experimental resolution. This could be expected since the phosphorus atoms are in an axial position and can therefore contribute to the σ^* molecular orbital via their $2p_z$ orbitals.

Experimental Section

The radical anion $[[CH_3N(PF_2)_2]_3(Co)_2(CO)_2]^-$ was prepared according to the previously described procedures.[11,17] X-Band ESR and ENDOR experiments were performed on a Bruker 220 D spectrometer equipped with a Bruker ENDOR accessory and an Oxford Instrument ESR 9 continuous-helium-flow cryostat. The extended Hückel calculations were performed using the ICON, version 8 program. The atomic orbitals are simple Slater-type orbitals except for cobalt 3d orbitals where a linear combination of two Slater functions was chosen. The parameters for all atoms used are listed in Table IV. The Wolfsberg–Helmholz proportionality constant k was set at 1.75.

Contribution from the Department of Chemistry, New Mexico State University, Las Cruces, New Mexico 88003

Kinetic Aspects of the Iron(III)- and Iron(II)-Tetrakis(*N*-methylpyridinium-4-yl)porphine Systems

G. A. Tondreau and R. G. Wilkins*

The spectra of monomeric and dimeric iron(III) and monomeric iron(II) complexes of TMPyP were examined (TMPyP = tetrakis(*N*-methylpyridinium-4-yl)porphine). The kinetics of interconversion of Fe(TMPyP)(OH)$^{4+}$ and (TMPyP)Fe-O-Fe-(TMPyP)$^{8+}$ have been studied by dilution relaxation at pH 7.0–8.5, I = 0.05 M, and 25 °C. The formation of the dimer is from Fe(TMPyP)(OH)$^{4+}$ and Fe(TMPyP)(H$_2$O)$_n{}^{5+}$ (k = 9 × 10^2 M^{-1} s^{-1}). Reduction of the iron(III)–TMPyP complexes by ascorbate is biphasic. The fast step leads to a bisadduct. The slow step is first-order (k = 4 × 10^{-3} s^{-1}), independent of ascorbate concentration. The reaction of Fe(TMPyP)$^{4+}$ with O$_2$ is third-order (k = 3.5 × 10^2 M^{-2} s^{-1}) and with H$_2$O$_2$ is second-order (k = 6.0 × 10^6 M^{-1} s^{-1}) at pH 8.0. The iron(II):oxidant mole ratio is 4:1 for O$_2$ and 2:1 for H$_2$O$_2$, and the product first formed is monomeric iron(III)–TMPyP. The mechanisms are discussed.

Introduction

The metalloporphyrin ring is an integral feature of a vast number of biological materials containing iron. There have therefore been a large number of studies of metal complexes of both naturally occurring porphyrins and synthesized derivatives.[1] The kinetics of substitution, redox, and photochemical reactions of metalloporphyrins have been amply studied,[2] and the results have relevance to the biological systems. Water solubility is conferred on the porphyrin by substituting hydrophilic cationic and anionic groups on the periphery of the porphyrin, and a number of these porphyrins and their metal complexes have been studied.[2]

We have previously examined the thermodynamic and kinetic aspects of the equilibrium between the monomer and dimer forms of the iron(III)–tetrakis(*p*-sulfonatophenyl)porphine complex (I,

X = CSO$_3{}^-$, ligand abbreviated TPPS).[3] In order to determine

I
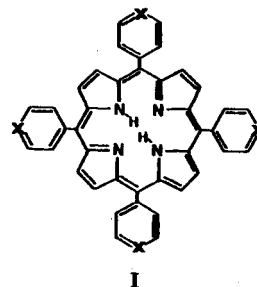
the effect of the porphyrin structure on this and other properties, we turn our attention to the iron–tetrakis(*N*-methylpyridinium-4-yl)porphine complex (I, X = NCH$_3{}^+$, ligand abbreviated TMPyP). The diagnosis of species present in iron(III) and iron(II) mixtures with TMPyP is difficult, and it is not surprising that

(1) *Porphyrins and Metalloporphyrins*; Smith, K. M., Ed.; Elsevier: Amsterdam, 1975. *The Porphyrins*; Dolphin, D., Ed.; Academic: New York, 1978. *Iron Porphyrins*; Lever, A. B. P., Gray, H. B., Eds.; Addison-Wesley: Reading, MA, 1983.
(2) Lavallee, D. K. *Coord. Chem. Rev.* **1985**, *61*, 55.
(3) El-Awady, A. A.; Wilkins, P. C.; Wilkins, R. G. *Inorg. Chem.* **1985**, *24*, 2053.

there is some disagreement as to the nature of the equilibria present.[4-8] We have reinvestigated the iron(III)–TMPyP system and measured the kinetics of monomer–dimer interconversion in the weakly basic region. We further describe the reduction of iron(III)–TMPyP by ascorbate[9] and the oxidation of the iron-(II)–TMPyP complex by oxygen and hydrogen peroxide. Here too, differences (as to the nature of the rate law) exist.[5,10,11]

Experimental Section

Materials. *meso*-Tetrakis(*N*-methylpyridinium-4-yl)porphine tetra-iodide was purchased from Strem Chemicals. The infrared spectrum indicated <5% non-methylated material.[11] The iron porphyrin chloride salt was used in all experiments, it being formed[4] by passing a slurry of the perchlorate salt[4,12,13] through a Dowex 1-X8 ion exchanger in the chloride form. The product was strongly hydrated.[4] Analyses indicated C:N:Cl ratios of 44:8.12:6.4. For both the monomer $C_{44}H_{36}FeN_8Cl_5$ and the dimer $(C_{44}H_{36}FeN_8)_2OCl_8$ the C:N ratio found is as expected, similar to those reported for laboratory-synthesized material.[4,8a,11a] Buffers used were as follows: 0.05 M 2-morpholinoethanesulfonic acid (Mes), pH 5.5–6.5; 0.05 M *N*-(2-hydroxyethyl)piperazine-*N'*-2-ethanesulfonic acid (Hepes), pH 7.0–8.0; 0.05 M 2-amino-2-(hydroxymethyl)-1,3-propanediol (Tris), pH 8.5–9.0. Outside these ranges, the pH was adjusted with acid or base. All chemicals used were the purest commercial products.

Spectra. The spectra of the iron(III) monomer were obtained at various pHs from an equilibrated solution (5–10 μM) of the solid. To obtain the iron(III) dimer spectrum, 10 mM of the equilibrated solution of the solid was diluted to $\sim$100 μM and the spectrum ran quickly (pH 8.0). The iron(II) spectrum was best obtained by adding an excess of ascorbate (2.5 mM) to an iron(III) solution (5–50 μM) until spectral changes were complete. The iron(III) porphyrin–ascorbate adduct was obtained by adding ascorbate (1–20 mM) to the porphyrin (10–100 μM), and the spectrum of this mixture was measured quickly. Unless otherwise specified, spectra were measured at pH 8.0, I = 0.10 M, and 25 °C, and 1- and 10-cm cells were used.

Fe(III) Monomer–Dimer Equilibrium. Spectral analysis of equilibrium solutions containing monomer and dimer ($\sim$100 μM total iron) provided equilibrium constants at pH 7.0–8.5 using the determined absorbance coefficient of the monomer and dimer. The kinetic experiments were carried out mainly by diluting a concentrated solution of the iron(III) solid ($\sim$5 mM) by 30–300-fold into the appropriate medium, quickly adjusting the pH when necessary, and observing the relaxation at 600 nm. In other experiments, the relaxation of a fresh solution of the solid (15 μM) or of a 100 μM solution of the freshly prepared monomer (from the iron(II) complex and O_2) was monitored. Relaxations were nicely first-order, and good agreement was observed in rate constants by the three approaches, for the same final conditions. Most measurements of the monomer–dimer equilibrium were at λ = 600 nm, I = 0.05 M. The monomer–dimer equilibration was complete within 60–90 min at pH 8.0 and within 10 min at pH 7.0.

Redox Experiments. The formation constant of the iron(III) porphyrin–ascorbate adduct was measured at pH 8.0 by treating the Fe(III) complex (10 μM) with increments of ascorbate (final concentrations 100 μM–1.7 mM) and measuring absorbances at 560–570 nm. All manipulations were carried out as quickly as possible. In the kinetics, iron(III) complex (10 μM) and ascorbate (5–20 mM) were mixed at pH 7.0 and 8.0 and absorbance changes monitored at 560 nm. All ascorbate reactions were at I = 0.1 M. Reaction stoichiometries for the oxidation reactions were obtained spectrally. Iron(II) porphyrin (100 μM prepared from 100 μM Fe(III) and 50 μM ascorbate in contact for 90 min) was titrated with O_2 (1.1 mM) or H_2O_2 (4.4 mM). The kinetics of the O_2 reaction were measured with use of 9.5–40 μM iron(II) porphyrin and
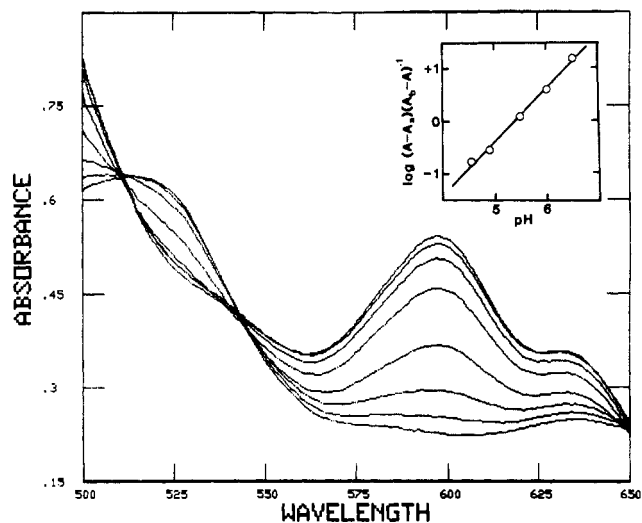
Figure 1. Spectra of iron(III)–TMPyP solutions (5.9 μM, I = 0.05 M) at pH 4.0, 4.6, 4.9, 5.5, 6.0, 6.5, 6.9, and 8.6 (increasing absorbance at 600 nm). The inset shows a plot of log $(A - A_a)(A_b - A)^{-1}$ vs. pH. A_a, A_b, and A are absorbances at 600 nm of acid, base, and equilibrium mixtures (slope = 1.05, pK_a = 5.5 ± 0.2, cell path 10.0 cm).
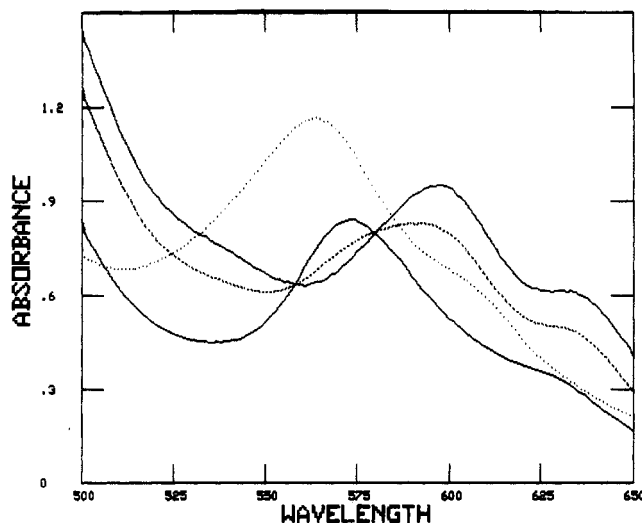
Figure 2. Spectra of Fe(TMPyP)(OH)$^{4+}$ (solid line with peak at 596 nm), (TMPyP)Fe-O-Fe(TMPyP)$^{8+}$ (solid line with peak at 574 nm), monomer/dimer equilibrium mixture (heavy dotted line), and Fe-(TMPyP)$^{4+}$ (light dotted line) (109 μM total iron, pH 8.0, I = 0.1 M, cell path 1.0 cm).

110–550 μM O_2 and with 0–17 μM Fe(III)–TMPyP present. The kinetics of H_2O_2 oxidation were determined with use of 2–10 μM Fe-(II)–TMPyP and 5–50 μM H_2O_2. All stoichiometrics and kinetics for the oxidation reactions were at pH 7.0 and 8.0 and I = 0.1 M with use of Hepes buffer and λ = 560 nm. All measurements were at 25 °C. Unless otherwise specified, all concentrations refer to the total iron content. Spectral and kinetic measurements were made with a Dionex stopped-flow apparatus or a Cary 14 spectrophotometer, both interfaced with an OLIS data collecting system.

Results

Iron(III)–TMPyP System. A solution of the iron(III) complex (5–10 μM) after standing for 1–2 h at pH 8.0 gave the spectra shown at various pHs (Figure 1). Isosbestic points at 513 and 540 nm were maintained between pH 4.0 and 8.6, strongly suggesting only two species were involved in this pH range. Analysis of the absorbances at 600 nm (Figure 1, inset), with consistent results at other wavelengths, indicates that one proton is involved in the interconversion and that the associated pK_1 = 5.5 ± 0.2 at I = 0.05 M. This is represented as in (1), any coordinated water

$$Fe(TMPyP)^{5+} \rightleftharpoons Fe(TMPyP)(OH)^{4+} + H^+ \quad K_1 \quad (1)$$

being omitted, the number being unknown with the acid 5+ form.[14]

(4) Pasternack, R. F.; Lee, H.; Malek, P.; Spencer, C. *J. Inorg. Nucl. Chem.* **1977**, *39*, 1865.

(5) Forshey, P. A.; Kuwana, T. *Inorg. Chem.* **1981**, *20*, 693.

(6) Kurihara, H.; Arifuku, F.; Ando, I.; Saita, M.; Nishino, R.; Ujimoto, K. *Bull. Chem. Soc. Jpn.* **1982**, *55*, 3515.

(7) Weinraub, D.; Peretz, P.; Faraggi, M. *J. Phys. Chem.* **1982**, *86*, 1839.

(8) (a) Kobayashi, N.; Koshiyama, M.; Osa, T.; Kuwana, T. *Inorg. Chem.* **1983**, *22*, 3608. (b) Kobayashi, N. *Ibid.* **1985**, *24*, 3324.

(9) Harris, F. L.; Toppen, D. L. *Inorg. Chem.* **1978**, *17*, 71, 74.

(10) Solomon, D.; Peretz, P.; Faraggi, M. *J. Phys. Chem.* **1982**, *86*, 1842.

(11) (a) Forshey, P. A.; Kuwana, T. *Inorg. Chem.* **1983**, *22*, 699. (b) Forshey, P. A.; Kuwana, T.; Kobayashi, N.; Osa, T. *Electrochemical and Spectrochemical Studies of Biological Redox Components*; Advances in Chemistry 201; American Chemical Society: Washington, DC, 1982; p 601.

(12) Hambright, P.; Fleischer, E. B. *Inorg. Chem.* **1970**, *9*, 1757.

(13) Neri, B. P.; Wilson, G. S. *Ann. N.Y. Acad. Sci.* **1973**, *206*, 568.

Table I. Spectral Characteristics of Fe(III)– and Fe(II)–TMPyP Complexes at pH 7.0–8.0

| | $10^{-4}\epsilon$, M^{-1} cm^{-1} | | | | | | | | |
complex	421 nm	423 nm	444 nm	558 nm	563 nm	574 nm	580 nm	596 nm	625–630 nm
(TMPyP)$_4$FeOFe(TMPyP)$_4^{8+}$	8.4[a]			1.16[b]		1.5[a]	1.5[b]		
Fe(TMPyP)(OH)$^{4+}$		9.5[a]		0.58[b]			0.76[b]	0.87[a]	0.57[c]
Fe(III)–TMPyP–ascorbate adduct			9.3		0.83				
Fe(TMPyP)$^{4+}$			14.0,[a] 16.0,[d]		1.1,[a] 1.3,[d]				
			16.0,[e] 11[f]		1.3[e]				

[a] Peak. [b] Isosbestic point for Fe(III) monomer, dimer. [c] Shoulder. [d] Reference 5. [e] Reference 7. [f] Reference 9.

Table II. Equilibria and Rate Constants for Monomer/Dimer Fe(III)–TMPyP Equilibria at $I = 0.05$ M

pH	k_f, M^{-1} s^{-1}	$10^{-8}k_f[H^+]^{-1}$, M^{-2} s^{-1}	k_r, s^{-1}	$10^{-5}k_r[H^+]^{-1}$, M^{-1} s^{-1}	$10^{-3}K_2$,[b] M^{-1}
7.0	21.2	2.1	1.0×10^{-2} (1.3×10^{-2}[a])	1.0	. 2.1 (2.6[c])
7.5	10.9	3.6	5.9×10^{-3}	2.0	1.9
8.0	2.8	2.8	1.1×10^{-3} (1.3×10^{-3}[a])	1.1	2.6 (3.4,[c] 2.0[c,d])
8.5	1.2	4.0	6.5×10^{-4}	2.2	1.9

[a] Complete dissociation of dimer at $I = 0.1$ M (NaCl).[9] [b] From k_f/k_r. [c] Spectral examination of equilibrated solution. [d] Reference 5.

Between pH 10 and 13 further spectral changes occur (not shown) with isosbestic points at 513, 540, 603, and 625 nm and a p$K \approx$ 11.5 can be assigned to an additional one-proton change. The remaining work on the system was confined to the pH 7.0–8.5 region. By equilibration of a concentrated solution (10 mM) of the iron(III) chloride salt, dilution to 100 μM with pH 8.0 buffer and rapid measurement, the spectrum of the dimer was obtained (Figure 2). If a 100 μM solution of the solid was prepared directly, the absorbance maximum was at 576 nm ($\epsilon = 1.4 \times 10^4$ M^{-1} cm^{-1}). The spectrum of the monomer was obtained by using $\leq$10 μM equilibrated solutions of the solid (Figure 2) or in more concentrated solution from O_2 oxidation of the Fe(II) porphyrin. The spectra of concentrated solutions of monomer and dimer changed slowly at pH 8.0, maintaining isosbestic points at 558 and 574 nm (Figure 2; also isosbestic points at 410, 443, and 461 nm (not shown)). The same final spectrum was obtained at equilibrium from both monomer- and dimer-containing solutions. Absorbance characteristics are shown in Table I.

Equilibrated solutions of known iron(III) content at pH 7.0 and 8.0 were spectrally analyzed at 535 and 600 nm for monomer content and the dimerization constant for (2) thus determined (Table II). The value of K_2 increased markedly with an increased

$$2Fe(TMPyP)(OH)^{4+} \rightleftharpoons$$
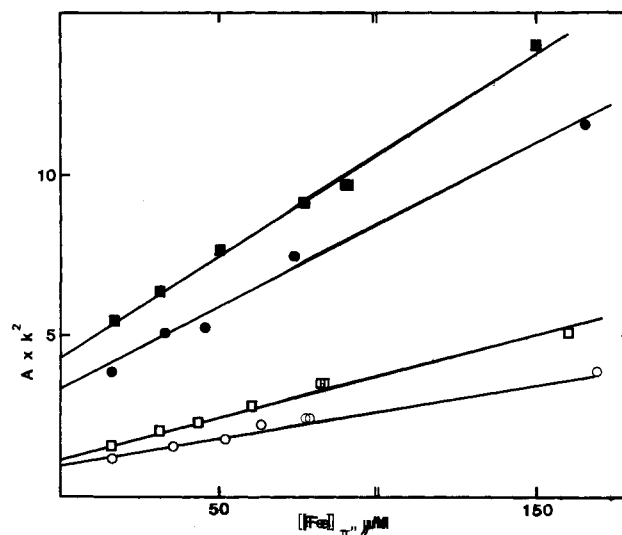$$(TMPyP)Fe-O-Fe(TMPyP)^{8+} + H_2O \quad k_2, k_{-2}, K_2 \quad (2)$$

ionic strength. The relaxation of a dimer-containing solution to a dimer/monomer mixture was nicely first-order. Most of the data were analyzed at 600 nm, but a similar result was obtained at 422 nm, although the absorbance changes were smaller. The observed relaxation rate constant, k, is related to the total iron concentration ($[Fe(III)]_T$) by expression 3.[15] Plots of k^2 vs.

$$k^2 = 8k_fk_r[Fe(III)]_T + k_r^2 \quad (3)$$

$[Fe(III)]_T$ for relaxations at pH 7.0–8.5 are shown in Figure 3 and lead to values of k_f and k_r, forward and reverse rate constants for dimerization at a specific pH, shown in Table II. A similar $k/[Fe(III)]_T$ correlation was observed for the relaxation of a monomer-containing solution.

Reduction of Fe(III)–TMPyP. Reduction of a iron(III) dimer/monomer equilibrium mixture by stoichiometric amounts or excess of ascorbate or dithionite gave finally a common spectrum (Figure 2). This was pH invariant between pH 5.5 and 8.0. Isosbestic points for iron(III) monomer and iron(II) product were at 430, 474, 515, and 587 nm, and for iron(III) dimer and iron (II) product transformation, isosbestic points were at 475, 515, and 623 nm (Table I).

(14) Ostrich, I. J.; Liu, G.; Dodgen, H. W.; Hunt, J. P. *Inorg. Chem.* **1980**, *19*, 619.
(15) Bernasconi, C. F. *Relaxation Kinetics*; Academic Press: New York, 1976; pp 14, 242.

Figure 3. Plots of relaxation rate constants, k, vs. total iron content, $[Fe]_T$, for Fe–TMPyP systems: (O) pH 7.0, $A = 10^4$; (●) pH 7.5, $A = 10^5$; (□) pH 8.0, $A = 10^6$; (■) pH 8.5, $A = 10^7$.

The reactions of a fresh (mainly dimer) or aged (monomer) solution with dilute dithionite solution was complete within mixing time ($\sim$1 ms). The reactions of both monomer and dimer with ascorbate at pH 7.0 and 8.0 were biphasic. The fast step can be assigned to the formation of an adduct. The analysis of spectral changes at 560–570 nm when iron(III) monomer (10 μM, pH 8.0, and $I = 0.10$ M) was treated with various concentrations of ascorbate (asc) and the absorbance measured within 1–2 min (before the slower stage starts) indicates that a bisadduct is formed (eq 4). The value of $K_4 = (2.4 \pm 0.5) \times 10^7$ M^{-2} at pH 8.0. The

$$Fe(TMPyP)(OH)^{4+} + 2asc^- \rightleftharpoons$$
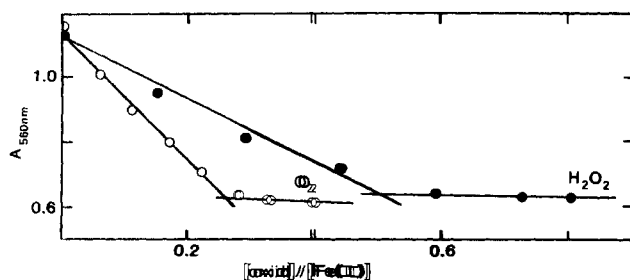$$Fe(TMPyP)(asc)_2^{3+} + OH^- \quad K_4 \quad (4)$$
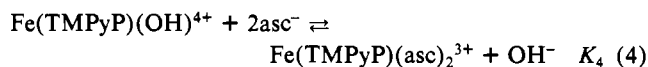
spectrum of the adduct was obtained by adding 1–20 mM ascorbate to the iron(III) complex and running the spectrum quickly (Table I). Isosbestic points at 430, 472, 505, and 630 nm were noted when the ascorbate adduct was transformed to the final iron(II) product. The slow change (4×10^{-3} s^{-1} at pH 8.0; 1.3 $\times 10^{-2}$ s^{-1} at pH 7.0) was independent of a change of concentration of ascorbate from 1 to 20 mM and of observation wavelengths of 560 and 445 nm. A fresh solution of the dimeric iron(III) complex gave similar behavior, that is, the formation of an adduct and a slow first-order change.

Oxidation of Fe(II)–TMPyP by O_2 and H_2O_2. Titration at pH 8.0 and $I = 0.10$ M of the Fe(II) complex with O_2 or H_2O_2 at 560 nm shows that 3.8 $\pm$ 0.2 and 2.0 $\pm$ 0.1 equiv of Fe(II) were oxidized by 1.0 equiv of O_2 and H_2O_2, respectively (Figure 4).

Figure 4. Titration at λ = 560 nm, pH 8.0, and I = 0.10 M of Fe-(TMPyP)$^{4+}$ with O_2 (O) and H_2O_2 (●). End points are at molar ratios of 0.26 (O_2-Fe(II)) and 0.50 (H_2O_2-Fe(II)). Solutions of 100 μM Fe(TMPyP)$^{4+}$ were prepared in both cases by reducing 100 μM Fe(III)-TMPyP with 50 μM ascorbic acid.

At 560 nm, the monomer–dimer equilibration is unaccompanied by an absorbance change and so the slow monomer–dimer change that occurs during the titration does not affect the result. The product of the oxidation in both cases is monomeric Fe(III) complex with characteristic peaks at 422 and 596 nm and isosbestic points between the Fe(II) reactant and Fe(III) product of 430 and 470 nm.

The kinetics of oxidation of Fe(II)-TMPyP with H_2O_2 were second-order (eq 5) with k_5 = (6.0 ± 0.3) × 10^6 M^{-1} s^{-1} at pH 8.0 and (3.5 ± 0.2) × 10^6 M^{-1} s^{-1} at pH 7.0 (I = 0.1 M in both cases). The loss of H_2O_2 (by Fe(III)-TMPyP catalysis, k = 1.3

$$-d[Fe(II)]dt = k_5[Fe(II)][H_2O_2] \qquad (5)$$

× 10^3 M^{-1} s^{-1} at pH 9)[11] is negligible during the oxidation. The delineation of the reaction order with the corresponding O_2 reaction presented problems. It was difficult to distinguish first-order from second-order loss of the Fe(II) complex in the presence of excess O_2. Further, the computed first- and second-order rate constants were both linearly dependent on the concentration of O_2 (110–550 μM). However, a second-order dependency was a better description for a change of initial Fe(II) concentration from 4.0 to 23 μM ([O_2] = 0.11 mM) since the reaction time (80% completion) decreased (from 0.22 to 0.04 s) with increasing initial concentration of Fe(II)-TMPyP. We conclude therefore that the rate law (6) best fits the kinetics of the O_2 reaction with k_6 = (3.5

$$-d[Fe(II)]/dt = k_6[Fe(II)]^2[O_2] \qquad (6)$$

± 0.5) × 10^2 M^{-2} s^{-1}, pH 7.0 and 8.0 (I = 0.1 M in both cases). An increase of Fe(III)-TMPyP concentration from zero to 17 μM at the beginning of the oxidation was without effect on the computed pseudo-second-order rate constant.

Discussion

Iron(III)-TMPyP System. It is very useful to characterize the species involved for interpreting the kinetics. Although it can be estimated that 10–100 μM solutions of the solid iron(III) complex will contain about 0.05–0.5 mM chloride ion, it is doubtful that chloride ion binds appreciably to the iron at these concentrations (see also ref 9). Significantly, some experiments with Fe-(TMPyP)(ClO$_4$)$_5$ as the source of iron(III) gave similar rate data. Since there is ambiguity on the ionization characteristics[4–8,11] a spectral/pH examination of the iron(III)-TMPyP complex was carried out, using an equilibrated dilute solution (>98% monomer) of the solid chloride (Figure 1). Two one-proton steps were indicated with pK = 5.5 ± 0.2 and ~11.5. In this regard, we agree with Kurihara et al.[6] and Kobayashi et al.,[8] who report pK's of 5.5, 5.7 and ~12 or 12.3, respectively, at I = 0.10 M from extensive spectral and MCD data. We formulate the first ionization as in (1). If the species present in the pH range of this study (7.0–8.5) were Fe(TMPyP)(OH)$_2$$^{3+}$ (see ref 4 and 13), the dimer would be formulated (HOFe(TMPyP))$_2$O and the kinetic data would refer to these species. Water-exchange experiments using oxygen-17 NMR do not allow the determination of the number of coordinated waters in the iron(III) acid form as 1 or 2,[14] nor do we know whether the hydroxo form is five- or six-coordinated. Further ionization (pK ≈ 11.5) probably[6,8] leads

to Fe(TMPyP)(OH)$_2$$^{3+}$. In our experiments at pH 7.0–8.5 we are therefore concerned with only one monomeric (monohydroxo) species. The agreement of the spectral characteristics of the monomer with those in the literature is excellent (Table I). At pH 8.3, the ratios of absorbance coefficients at 421, 600, and 638 nm are 1.0:1.6:17.6 compared with 1.0:1.7:18[4] and 1.0:1.5:19.[13] The "best" spectrum of the dimer at pH 7–8 was obtained by equilibrating a concentrated solution of the solid chloride (at high concentrations and high ionic strength the dimerization constant is large) and then rapidly diluting and measuring the spectrum (Figure 2). Even with these conditions, we are uncertain that dimerization is 100% complete (however, see below). Surprisingly, we found that the solid chloride is substantially in the *dimeric* form, as evidenced from the spectral characteristics of a fresh dilute solution of it. Most workers have used the iron(III) perchlorate salt, and analysis of this indicates it is monomeric Fe-(TMPyP)(ClO$_4$)$_5$.[12] Analyses of our chloride salt indicated chloride ion contamination, and we were unable to differentiate the monomer (Fe:Cl = 1:5) and dimer (Fe:Cl = 1:4) by analyses. Previously reported[5,9] maxima for the dimer[5,9] are at wavelengths slightly higher than 574 nm, and presumably these solutions contain small amounts of monomer.

The spectrum of a dimer solution or of a concentrated monomer solution (prepared by oxidizing Fe(II)-TMPyP with O_2) changes slowly, and for example at 100 μM total iron, pH 8.0, and I = 0.05 M a common equilibrium spectrum of a monomer/dimer mixture is attained (Figure 2). This inherent slowness in monomer/dimer equilibration has been previously noted.[5,6,9] The relaxation obeyed first-order kinetics, even although the perturbations were in some conditions quite large. Although surprising at first, it is now clear that relatively large perturbations can still produce first-order relaxation kinetics.[15–17] With a monomer/dimer equilibrium, combination of a relatively low dimerization constant and a low concentration allows for large deviations but still a relaxation treatment.[17] It can be estimated that with [iron]$_T$ = 35 μM and K_2 = 2 × 10^3 M^{-1}, a 45% change in the concentration of one of the species is allowable before deviation from first-order kinetics *begins*.[17] One safeguard is to process the latter portion only of the relaxation curve (which corresponds to a smaller perturbation), but in our case, this was unnecessary. The dimerization constant K_2 obtained from the rate data does not vary from pH 7.0 to 8.5 (Table II), which indicates that in this region no protons are involved, and we formulate the dimerization as in (2), with the dimer containing an oxy bridge. The latter formulation is suggested by a change from high spin to low spin as acidic monomer is converted to basic dimer.[18] For the equilibrium (7) between acid monomer and dimer, K_7 = K_2K_1^{2} = 1.8 × 10^{-8}

$$2Fe(TMPyP)^{5+} \rightleftharpoons$$
$$(TMPyP)Fe-O-Fe(TMPyP)^{8+} + 2H^+ \qquad K_7 \quad (7)$$

M. This value is quite close to that obtained for the TPPS system (0.79 × 10^{-8} M).[19] The agreement of K_2 from kinetic data with that obtained from spectra of equilibrated solutions (Table II) indicates that (a) the relaxation approach is valid and (b) the dimer spectrum is substantially correct, since a knowledge of absorbance coefficient of monomer and dimer is required to determine K_2 from spectral measurements but not from kinetic data.
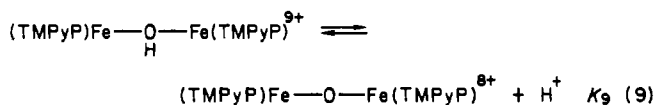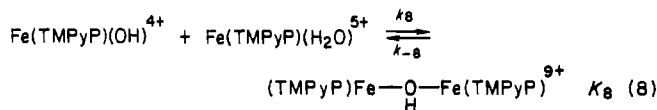
The rate constants k_f and k_r are both linearly dependent on [H$^+$] concentration (Table II). This relationship has been previously observed for k_r, when *complete* dissociation of the dimer was measured.[9] Our values for k_r are in good agreement with those previously reported[9] (Table II). A suggested mechanism[9] consistent with our more detailed findings is given by (1), (8), and (9). In the pH region 7.0–8.5, where K_1 > [H$^+$], it is easily shown

(16) Hiromi, K. *Kinetics of Fast Enzyme Reactions*; Wiley: New York, 1979; p 198.
(17) Brouillard, R. *J. Chem. Soc., Faraday Trans. 1* **1980**, *76*, 583.
(18) Goff, H.; Morgan, L. O. *Inorg. Chem.* **1976**, *15*, 3180.
(19) Fleischer, E. B.; Palmer, J. M.; Srivastava, T. S.; Chatterjee, A. *J. Am. Chem. Soc.* **1971**, *93*, 3162.

$$Fe(TMPyP)(OH)^{4+} + Fe(TMPyP)(H_2O)^{5+} \underset{k_{-8}}{\overset{k_8}{\rightleftharpoons}}$$

$$(TMPyP)Fe\!-\!\underset{H}{O}\!-\!Fe(TMPyP)^{9+} \quad K_8 \quad (8)$$

$$(TMPyP)Fe\!-\!\underset{H}{O}\!-\!Fe(TMPyP)^{9+} \rightleftharpoons$$

$$(TMPyP)Fe\!-\!O\!-\!Fe(TMPyP)^{8+} + H^+ \quad K_9 \quad (9)$$

$$k_8 = k_f K_1 / [H^+] \qquad (10)$$

that for dimerization the simple observed relationship (10) holds. From $k_f[H^+]^{-1} = (3.1 \pm 1.0) \times 10^8 \ M^{-2} \ s^{-1}$ the calculated value of k_8 is $(9 \pm 3) \times 10^2 \ M^{-1} \ s^{-1}$ and it can be estimated that $k_2 \ll 1 \ M^{-1} \ s^{-1}$. The enhanced reactivity ($>10^3$-fold) for the combination of one aqua and one hydroxo iron(III) monomer over that of two hydroxo species has been previously observed with the Fe(III)–TPPS system,[3] for which the corresponding rate constants are $1.5 \times 10^6 \ M^{-1} \ s^{-1}$ and $\ll 10^4 \ M^{-1} \ s^{-1}$. The enhanced reactivity for the TPPS system may reside in a higher water-exchange lability,[14] since the latter process has been proposed to control dimer formation with iron(III) complexes.[20,21]

By examining the breakdown of the dimer over a wide range of pH, the values of k_{-8} and K_9 were determined by Harris and Toppen.[9] In the pH region we examined, $[H^+] < K_9$ and relationship 11 applies. Our value of $k_r[H^+]^{-1}$, $(1.6 \pm 0.6) \times 10^5$

$$k_{-8} = k_r K_9 / [H^+] \qquad (11)$$

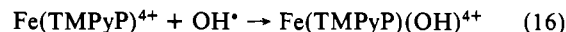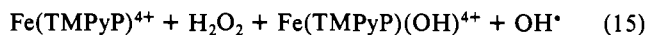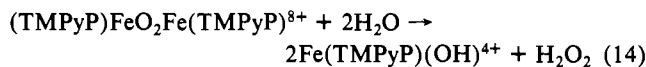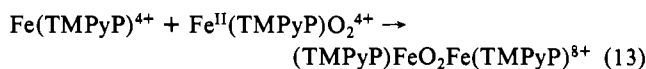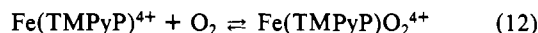$M^{-1} \ s^{-1}$, is in good agreement with that of $k_{-8}K_9^{-1}$, found[9] as $1.2 \times 10^5 \ M^{-1} \ s^{-1}$.

Redox Reactions. The characteristics of the common spectrum of the iron(II)–TMPyP product of reduction of monomeric or dimeric Fe(III)–TMPyP by ascorbate or dithionite are similar to those reported (Table I). The iron(II) product undergoes no spectral changes between pH 5.5 and 8.0. This behavior is consistent with a reported $pK \approx 11$,[6,8] and the iron(II) species is assumed to be *monomeric* Fe(TMPyP)(OH$_2$)$_2^{4+}$ (see also ref 5). The reduction of monomer or dimer by dithionite is too fast to measure by stopped-flow, and this is consistent with a reported second-order rate constant $\sim 3 \times 10^7 \ M^{-1} \ s^{-1}$ for reduction of Fe(III)–TMPyP by O_2^- ion.[22] It is generally found that rate constants for reduction by SO_2^- are 10^2–10^3 larger than by O_2^- ion.[23] No slow reduction of the dimer by dithionite, controlled by its dissociation, is observed, unlike the case with the TPPS complex.[3] Reduction by ascorbate is markedly biphasic, analysis of which indicates the rapid formation of a common 2:1 ascorbate–Fe(III) adduct, the kinetics of which were not investigated, and a slower ($\sim 10^{-2} \ s^{-1}$) first-order formation of the final product. This latter process is independent of ascorbate concentration. It is tempting to assign the slow change to an intramolecular electron transfer within the adduct. However, the possibility remains that the adduct is a dead-end complex. The formation of a 2:1 adduct (rather than a 1:1 adduct) has precedence with the imidazole and histidine derivatives of Fe(III)–TMPyP[7] and with the imidazole, histidine, and pyridine derivatives of Fe(III)–TPPS.[24] In addition, a common monomeric adduct results from the addition of the ligands to monomer or dimer forms of the Fe(III) porphyrins.[7,24] The stability of the bis(ascorbate) adduct $(2.4 \pm 0.5) \times 10^7 \ M^{-2}$ is somewhat larger than those of the other mentioned complexes (10^3–$10^6 \ M^{-2}$). Our kinetic observations differ from those reported by Harris and Toppen for the reduction in the pH 4–7 range.[9] In that study a single step only was observed and in the presence

of excess ascorbate the loss of Fe(III) was second order. A mechanism was suggested invoking preferential reduction of the dimer in equilibrium in small amounts with the monomer. There is no evidence in our study for enhanced reactivity of dimer over monomer toward ascorbate in the pH range 7–8.

The ability of FeTMPyP to reduce O_2 quantitatively to H_2O at pH 1.5–11.0 has been previously demonstrated by thin-layer-cell coulometry.[11] In agreement, our spectral titrations indicate a 4:1 and 2:1 stoichiometry respectively for O_2 and H_2O_2 oxidations of Fe^{II}TMPyP (Figure 4). A third-order rate law has been suggested for the oxygen reaction with Fe(TMPyP)$^{4+}$ from pulse radiolysis studies, but no rate constants were cited.[10] On the other hand, a second-order rate law has also been reported for this reaction.[5,11] It is quite difficult in some instances to distinguish pseudo-first-order from pseudo second-order kinetics.[25] We favor the latter for the reasons given and therefore an overall third-order rate law (6). If we assumed a second-order rate law, the rate constant $\sim 2 \times 10^5 \ M^{-1} \ s^{-1}$ at pH 8 is decidedly lower than that reported $((4–5) \times 10^7 \ M^{-1} \ s^{-1}$ at pH 9).[5,11]

The stoichiometries and rate laws for the oxidation of the Fe(II)– to the Fe(III)–TMPyP complex by O_2 and by H_2O_2 are consistent with the mechanism given by (12)–(16), in which possible coordinated waters are omitted. Step 13 is the rate-

$$Fe(TMPyP)^{4+} + O_2 \rightleftharpoons Fe(TMPyP)O_2^{4+} \qquad (12)$$

$$Fe(TMPyP)^{4+} + Fe^{II}(TMPyP)O_2^{4+} \rightarrow$$
$$(TMPyP)FeO_2Fe(TMPyP)^{8+} \quad (13)$$

$$(TMPyP)FeO_2Fe(TMPyP)^{8+} + 2H_2O \rightarrow$$
$$2Fe(TMPyP)(OH)^{4+} + H_2O_2 \quad (14)$$

$$Fe(TMPyP)^{4+} + H_2O_2 + Fe(TMPyP)(OH)^{4+} + OH^\bullet \qquad (15)$$

$$Fe(TMPyP)^{4+} + OH^\bullet \rightarrow Fe(TMPyP)(OH)^{4+} \qquad (16)$$

determining step in the overall oxidation of four molecules of Fe(TMPyP)$^{4+}$ by one oxygen molecule, since this reaction is third-order. This leads to the observed rate law (6), with (12) present as a labile preequilibrium. Step 12 would be rate-determining if a second-order rate law were obeyed.[11] Step 12, as written, is preferred to the intermolecular electron transfer (17),

$$Fe(TMPyP)^{4+} + O_2 + OH^- \rightleftharpoons Fe(TMPyP)(OH)^{4+} + O_2^-$$
$$(17)$$
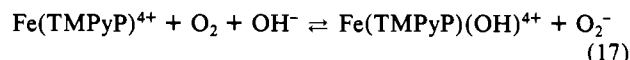
since there is no effect of changing concentrations of the Fe(III) product on the rate of the O_2 reaction. The steps (14)–(16) subsequent to the rate-determining step are considered rapid. The last two steps can be so demonstrated, by the observation of a rapid second-order oxidation of Fe(TMPyP)$^{4+}$ by H_2O_2. It is easily demonstrated that even with the low concentrations of H_2O_2 produced, the time frame of step 15 is shorter than that of (12) plus (13). An iron(III)–peroxide intermediate has been preferred for step 15, this then reacting with another iron(II) to give the iron(III) product.[11]

The slow monomer/dimer equilibration at pH 8.0 allows the assignment of the monomer as the *immediate* product of the oxygen reaction. This has been suggested by previous workers.[5,9,24] This observation also indicates that the iron(II)–TMPyP complex is monomeric in the conditions of the oxidation. This behavior contrasts with that of the oxygen reactions of iron(II) porphyrins signified (P) in noncoordinating solvents such as toluene. Here, usually, the product is the iron(III) dimer formed in a series of steps from the peroxo-bridged intermediate (P)FeO$_2$Fe(P). By working at low temperatures (−70 °C), it has been possible to identify the oxygen adduct, the peroxo-bridged intermediate, and Fe(IV) species as intermediate in the oxidation of various iron(II) porphyrins by O_2.[26] The lack of a dimer product from the O_2

(20) Eigen, M.; Wilkins, R. G. *Mechanisms of Inorganic Reactions*; Advances in Chemistry 49; American Chemical Society: Washington, DC, 1965; p 55.
(21) Wilkins, R. G.; Yelin, R. E. *Inorg. Chem.* **1969**, *8*, 1470.
(22) Ilan, Y.; Rabani, J.; Fridovich, I.; Pasternack, R. F. *Inorg. Nucl. Chem. Lett.* **1981**, *17*, 93.
(23) Bradič, Z.; Wilkins, R. G. *J. Am. Chem. Soc.* **1984**, *106*, 2236.
(24) Fleischer, E. B.; Fine, D. A. *Inorg. Chim. Acta* **1978**, *29*, 267.

(25) Scott, R. A.; Gray, H. B. *J. Am. Chem. Soc.* **1980**, *102*, 3219.
(26) Balch, A. L.; Chan, Y.-W.; Cheng, R.-J.; La Mar, G. N.; Latos-Grazynski, L.; Renner, M. W. *J. Am. Chem. Soc.* **1984**, *106*, 7779 and references therein.

reaction with Fe(TMPyP)$^{4+}$ suggests that an Fe(IV) species is not an intermediate.

Contribution from the Institut de Chimie minérale et analytique, Université de Lausanne, Place du Château 3, CH-1005 Lausanne, Switzerland

FT IR Investigation of the Interaction between Perchlorate and Trivalent Neodymium, Europium, Terbium, and Erbium Ions in Anhydrous Acetonitrile[1,2]

Jean-Claude G. Bünzli* and Catherine Mabillard

The interaction between perchlorate and Nd(III), Eu(III), Tb(III), and Er(III) ions has been investigated in anhydrous CH$_3$CN and CD$_3$CN. Vibrations due to unassociated (u), monodentate (m), and bidentate (b) perchlorate ions could be identified in 0.05 M solutions of Ln(ClO$_4$)$_3$. Quantitative FT IR measurements allowed the determination of the number of ClO$_4^-$(u) ions per Ln(III) ion, n_u, which is equal to 1.82 (Nd), 2.13 (Eu), 2.11 (Tb), and 2.07 (Er). This is in agreement with conductometric data that correspond to 2:1 electrolytes. The proportion of ClO$_4^-$(b) is low, between 5 and 10% of the total perchlorate concentration, whereas the proportion of ClO$_4^-$(m) varies from 39% (Nd) to ca. 22 ± 4% for Eu, Tb, and Er. The influence of the solvent on the concentration of the various perchlorate species has also been determined. For Eu, n_u = 1.5 in acetone and 2.4 in methanol. The proportion of ClO$_4^-$(b) is much lower in these two solvents than in acetonitrile. Inner-sphere Ln(III)/ClO$_4^-$ interactions consistent with these findings are proposed. Therefore, the data reported in this study indicate that the solutions contain the lanthanide species [Ln$_{solv}$]$^{3+}$, [LnClO$_4$(m)$_{solv}$]$^{2+}$, [LnClO$_4$(b)$_{solv}$]$^{2+}$, and [Ln(ClO$_4$)$_2$(m and/or b)$_{solv}$]$^+$. Their concentrations are evaluated as well as the apparent equilibrium ratio for the monoperchlorato species: log K_1 (±0.5) = 1.8, 1.9, and 2.1 for Ln = Eu, Tb, and Er. A difference is observed between the behavior of Nd(III) and that of the other Ln(III) ions included in this report.

Introduction

Trivalent lanthanide complexes and solvates are dominated by strong ion–dipole interactions and therefore do not display the restricted stereochemistry typical of the d transition elements. The number and arrangement of the ligand donor atoms in the primary coordination sphere are the result of the interplay between steric and electrostatic factors,[4] and coordination numbers ranging from 3 to 14 have been reported in the solid state.[5,6] In solution, despite almost 3 decades of research, many aspects of the coordination chemistry of these metal ions remain unclear. In particular, the questions of an eventual coordination change within the 15-element series or of the exact bonding mode (i.e. inner or outer sphere) for specific ligands are still open. Since the lanthanide ions are being increasingly used as spectroscopic probes in biochemistry,[7,8] more basic information is needed. The field has been recently reviewed,[9,10] and the use of modern instrumentation has enabled the acquisition of valuable data, especially in water[11] and in aqueous organic solvents.[12,13] In previous parts of this series of papers, we have tried to determine the coordination numbers of some Ln(III) ions (Ln = Nd, Eu, Tb, Er) in anhydrous solutions of weakly coordinating organic solvents.[3,14–18] In particular, we have addressed the problem of perchlorate coordination to europium ion in acetonitrile solutions and were able to prove by FT IR spectrometry that some degree of inner-sphere coordination occurs.[14] In this paper, we extend our vibrational study to lighter (neodymium), intermediate (terbium), and heavier (erbium) lanthanide ions in order to investigate whether differences appear in their solution behavior when the ionic radius is varied. New data for europium perchlorate are also provided.

Experimental Part

Lanthanide perchlorates were prepared from the 99.99% pure oxides (Glucydur) and reagent grade perchloric acid (Merck). Complete dehydration of the salts was performed at 60–110 °C, under reduced pressure, 10^{-5} mmHg, during 10–12 days. Analytical grade silver perchlorate (Merck) was used after drying at 90–110 °C. Acetonitrile (Fluka) and deuterated acetonitrile (99.8%, Ciba-Geigy) were treated with CaH$_2$ and P$_4$O$_{10}$ and distilled. The solutions were prepared under a strictly controlled atmosphere of N$_2$, with less than 10 ppm water, and contained less than 0.1 molecule of water per Ln(III) ion. In a few cases, the solutions had to be filtered to eliminate traces of insoluble oxychlorides generated during the dehydration of the perchlorates. The lanthanide ion concentration was determined by complexometric analysis with Ti-

(1) FT IR and Fluorometric Investigation of Rare-earth and Metallic Ion Solvation. 7. For part 6: see ref 3.
(2) Abstracted, in part, from the Ph.D. Thesis of C.M.; for a preliminary report, see ref 4.
(3) Bünzli, J.-C. G.; Vuckovic, M. M. *Inorg. Chim. Acta* **1984**, *90*, 105–12.
(4) Bünzli, J.-C. G.; Mabillard, C. *J. Less-Common Met.* **1983**, *94*, 317–18.
(5) Thompson, L. C. In *Handbook on the Physics and Chemistry of Rare Earths*; Gschneidner, K. A., Jr., Eyring, L., Eds.; North-Holland: Amsterdam, 1979; Chapter 25.
(6) Jørgensen, C. K. In *Handbook on the Physics and Chemistry of Rare Earths*; Gschneidner, K. A., Jr., Eyring, L., Eds.; North-Holland: Amsterdam, 1979; Chapter 23.
(7) Horrocks, W. DeW., Jr.; Albin, M. *Prog. Inorg. Chem.* **1984**, *31*, 1–104.
(8) Albin, M.; Horrocks, W. DeW., Jr. *Inorg. Chem.* **1985**, *24*, 895.
(9) Choppin, G. R. *J. Less-Common Met.* **1984**, *100*, 141.
(10) Lincoln, S. F. In "Advances in Inorganic and Bioinorganic Mechanisms"; Sykes, A. G., Ed.; Academic: London, 1986; Vol. 4, pp 217–287.
(11) Habenschuss, A.; Spedding, F. H. *J. Chem. Phys.* **1980**, *73*, 442.
(12) Brücher, E.; Glaser, J.; Grenthe, I.; Puigdomenech, I. *Inorg. Chim. Acta* **1985**, *109*, 111.
(13) Silber, H. B. *J. Less-Common Met.* **1985**, *112*, 207–33.
(14) Bünzli, J.-C. G.; Yersin, J.-R.; Mabillard, C. *Inorg. Chem.* **1982**, *21*, 1471–6.
(15) Bünzli, J.-C. G.; Mabillard, C.; Yersin, J.-R. *Inorg. Chem.* **1982**, *21*, 4214–18.
(16) Bünzli, J.-C. G.; Yersin, J.-R. *Helv. Chim. Acta* **1982**, *65*, 2498–506.
(17) Bünzli, J.-C. G.; Vuckovic, M. M. *Inorg. Chim. Acta* **1983**, *73*, 53–61.
(18) Bünzli, J.-C. G.; Yersin, J.-R. *Inorg. Chim. Acta* **1984**, *94*, 301–8.